Electrochemical Performance of Sol-Gel Synthesized $LiFePO_4$ in Lithium Batteries

Yaoqin Hu,* Marca M. Doeff,* Robert Kostecki,† and Rita Fiñones*

*Materials Sciences Division

and

†Environmental Energy Technologies Division

Lawrence Berkeley National Laboratory

University of California

Berkeley, CA 94720, USA

This work was supported by the Assistant Secretary for Energy Efficiency and Renewable Energy, Office of FreedomCAR and Vehicle Technologies of the U.S. Department of Energy under Contract No. DE-AC03-76SF00098. Y. H. would like to thank the Department of Chinese Education for financial support. Some of this work was previously presented as Abstract 121 at the 202nd Meeting of the Electrochemical Society, Salt Lake City, UT October 2002.

Abstract

$LiFePO_4$, $Li_{0.98}Mg_{0.01}FePO_4$, and $Li_{0.96}Ti_{0.01}FePO_4$ were synthesized via a sol-gel method, using a variety of processing conditions. For comparison, $LiFePO_4$ was also synthesized from iron acetate by a solid state method. The electrochemical performance of these materials in lithium cells was evaluated and correlated to mean primary particle size and residual carbon structure in the $LiFePO_4$ samples, as determined by Raman microprobe spectroscopy. For materials with mean agglomerate sizes below 20 μm, an association between structure and crystallinity of the residual carbon and improved utilization was observed. Addition of small amounts of organic compounds or polymers during processing results in carbon coatings with higher graphitization ratios and better electronic properties on the $LiFePO_4$ samples and improves cell performance in some cases, even though total carbon contents remain very low (<2%). In contrast, no performance enhancement was seen for samples doped with Mg or Ti. These results suggest that it should be possible to design high power $LiFePO_4$ electrodes without unduly compromising energy density by optimizing the carbon coating on the particles.

Introduction

$LiFePO_4$ is an attractive candidate for use as a cathode material in lithium ion batteries based on environmental and safety considerations.[1, 2] Unfortunately, poor rate capability makes it difficult to utilize $LiFePO_4$ electrodes fully in lithium cells at room temperature unless modifications are made to the material to ameliorate the low intrinsic electronic conductivity and slow lithium ion diffusion across the $LiFePO_4/FePO_4$ boundary.[3] Recently, improvements have been made to $LiFePO_4$ through optimization of

synthesis techniques to minimize the particle size without compromising purity,[4,5,6] doping to improve the intrinsic conductivity,[7] addition of metal or carbon particles during synthesis[8] or incorporating organic or polymeric additives to form conductive carbon coatings on the particles during firing.[9,10] Unfortunately, small particle sizes and even relatively small amounts of conductive additives reduce the tap density and volumetric energy density to a level that may make $LiFePO_4$ impractical for many common battery applications.[11] Strategies such as the ones described above to improve power density should be optimized to avoid unduly compromising energy density. To accomplish this, it is necessary to gain a complete understanding of synthesis conditions that affect the performance of $LiFePO_4$. Sol-gel synthesis is particularly well-suited to such a study, because it results in very pure materials with well-controlled particle sizes, and additives can be readily incorporated prior to firing.

Experimental

$LiFePO_4$ samples were made by a solid-state reaction and by a sol-gel process. For the solid state method, a modification of the procedure of Yamada et al. was used.[4] Li_2CO_3 (lithium carbonate, Mallinckrodt), $Fe(CH_3COO)_2$ $2H_2O$ (iron acetate, Aldrich) and $(NH_4)H_2PO_4$ (Dihydrogen ammonium phosphate, EM Sciences) were planetary milled in acetone and mixed thoroughly under N_2 to avoid oxidation. The mixture was then heated at 2º/min to 300°C under flowing N_2 for ten hours to decompose the acetate and phosphate. The powder was then ground again in a planetary ball mill for 30 minutes and heated to 600°C under flowing N_2 gas for eight hours.

For sol-gel samples, the starting materials were $Fe(NO_3)_3 \cdot 9H_2O$ (iron nitrate, Aldrich), $Li(CH_3COO) \cdot 2H_2O$ (lithium acetate, Aldrich), H_3PO_4 (phosphoric acid, Sigma)

and $HOCH_2COOH$ (glycolic acid, Aldrich). For doped samples, 2 mol % of the lithium acetate was replaced by 1 mol % $Mg(NO_3)_2.6H_2O$ (magnesium nitrate, EM Sciences) or 4 mol % lithium acetate was replaced by 1 mol % $Ti(OCH_2CH_3)_4$ (titanium ethoxide). The metal compounds were first dissolved in phosphoric acid and de-ionized water. This solution was mixed until homogeneous and glycolic acid was added while stirring, until the molar ratio of glycolic acid to metal ions was 2:1. Ammonium hydroxide was added to the solution to adjust the pH to between 8.5 and 9.5. The solution was then heated to 70-80°C under N_2 until a gel formed. For most samples, the gel was transferred to an alumina boat and heated at 2º/min to 500ºC under flowing N_2, and was decomposed at that temperature for ten hours. The resultant powders were then ground and heated at a rate of 2º/min to 600ºC or to 700ºC under a flow of N_2 gas, for various lengths of time. Table 1 lists the processing conditions for the solid state sample (designated 3A) and the sol-gel samples (designated by batch numbers and the letters SG). For some samples made the same way as 7SG, organic compounds were added during the intermediate grinding step, prior to final firing at 600ºC, in an amount equivalent to 2 wt% C in the mix. These are listed in Table 2, and designated by a batch number and the letter C.

A Siemens D5000 diffractometer was used to obtain x-ray powder diffraction patterns on the samples, using Cu Kα radiation (λ=1.54A). Particle sizes were determined with a Beckman Coulter particle size analyzer (model LS 230, with small volume module), and a scanning electron microscope (ISI-DS 130C dual stage) was used to observe the particle morphologies. Elemental carbon, nitrogen, and hydrogen analyses on samples were performed by Luvak Inc. (Boylston, MA).

An integrated Raman microscope system "Labram" made by ISA Groupe Horiba was used to analyze the structure and composition of individual particles of $LiFePO_4$. The excitation wavelength was supplied by an internal He-Ne (632 nm) 10 mW laser. The power of the laser beam was adjusted to 0.1 mW with neutral filters of various optical densities. The size of the laser beam at the sample was ~1.2 μm. Baseline correction and deconvolution analysis was performed with a commercial software package (PeakFit, version 4.05, SPSS Inc.).

Laminated electrodes containing 80 wt.% active material, 8 wt.% Kynar PVdF binder, 6 wt.% SFG-6 synthetic flake graphite (Timcal Ltd., Graphites and Technologies) and 6 wt% compressed acetylene black were prepared by spreading a slurry in N-methyl methylpyrrolidone onto aluminum foil current collectors and allowing them to dry. A small amount of Pelseal Bonding Agent 65 (Pelseal Technologies, LLC) was also added to the slurry, according to the manufacturer's directions, to prevent cracking. Electrodes were dried overnight in air and then in a 120°C vacuum oven for at least 8 hours. For coin cells with lithium anodes, 5/8'' diameter electrodes were punched out and weighed individually to determine loading. This was typically 5-15 mg/cm^2 of active material. 2032 size coin cells were assembled in an helium-filled glove-box, using lithium metal as a counter electrode and 1M $LiPF_6$ in 1:2 ethylene carbonate/dimethyl carbonate (EC/DMC). At least two of each type of cell was assembled, and the performances were compared to ensure good reproducibility of results.

Cells were cycled galvanostatically between 2.5 and 3.9 V at room temperature, using a Macpile II galvanostat/potentiostat (Bio-Logic, SA, Claix, France). Cyclic

voltammetry (CV) experiments were carried out using an Arbin BT/HSP-2043 battery cycler.

Results and Discussion

All materials give x-ray diffraction patterns consistent with $LiFePO_4$ (or substituted variants) and are phase-pure. No lithium-containing impurities were detected by ^{7}Li-MAS NMR, and signals were identical for all of the materials that were examined.[12] We found that all $LiFePO_4$ samples contained elemental carbon as an impurity, which originated from the carbon-containing precursor compounds. The residual carbon content never exceeded 2% (see Table 3), much below the total carbon amount in the acetate and carbonate precursors. Most of the carbon originating from acetates and carbonates is released as gaseous products during calcination. More residual carbon is detected in 3A than in the sol-gel samples because of the larger amount of carbon in the precursors. (3A was also a darker gray in color than the sol-gel samples, which were light to medium gray) The residual carbon content of the sol-gel samples does not bear any obvious relationship to the heating regime, i.e., duration and temperature of the heat-treatment.

Doped samples 14SGA, 14SGB ($Li_{0.98}Mg_{0.01}FePO_4$) and 16SG ($Li_{0.96}Ti_{0.01}FePO_4$) were prepared similarly to 7SG, and were light in color. This is consistent with their low carbon content (Table 3), and suggests that the intrinsic electronic conductivity of these materials is not significantly better than that of undoped $LiFePO_4$.

Figure 1 shows scanning electron micrographs of several of the powders. The solid state processed material, 3A, consists of small irregularly shaped particles that appear larger than those of the sol-gel prepared 7SG. The particle morphology of 7SG,

small flakes of varying sizes, is representative of sol-gel samples heated at 600 ºC and subjected to an intermediate grinding step. There is little particle growth at this temperature, and the morphology changes only slightly with increased heating time. In contrast, heating at 700 ºC causes the flakes to fuse together partially to form large porous agglomerates (samples 6SG and 8SG in Figures 2c and 2d), regardless of the method of grinding or grinding time after the decomposition step. This also occurred to some extent to the sample heated directly to 600 ºC without an intermediate grinding step (3SG), although the effect was less pronounced. The size of the small flakes in the sol-gel prepared materials is not substantially affected by changes in processing, although the size of the agglomerates is.

Figure 2 shows cyclic voltammograms of lithium coin cells containing $LiFePO_4$ composite electrodes. The cathodes exhibited oxidation peaks at 3.5-3.7 V and distinct reduction peaks at 3.2-3.3 V, consistent with a two-phase redox reaction at about 3.45 V vs. Li/Li^+. The peak intensities vary for the different cathode samples. Capacities calculated from the peaks in the CV experiments are similar to those obtained during galvanostatic cycling at low to moderate discharge rates (<C/5). Capacities of cathodes containing large agglomerates show an inverse relationship with the size (Figure 3). Electrochemical activity could be improved significantly in some cases by planetary milling powders after the final firing (compare 9SG and 10SG). However, utilization did not necessarily increase to values obtained for materials with inherently small particle sizes after calcination. Because of the poor electrochemical performance of cathodes that contained large $LiFePO_4$ particles, we limited the rest of our investigations to powders with mean agglomerate sizes below about 20 μm.

Galvanostatic discharges at 0.027 mA/cm^2 of Li/1M $LiPF_6$, EC-DMC/$LiFePO_4$ cells for selected $LiFePO_4$ powders are shown in Figure 4. The two materials with the highest residual carbon contents, 3A and 7SG, also had the highest discharge capacities and best rate capabilities (Figures 5a and b), but for other samples, electrochemical performance did not track carbon content. A recent Raman microprobe spectroscopic investigation of these powders[13] indicates that the structure of the residual carbon on the $LiFePO_4$ particles is extremely important for electrochemical performance. Specifically, better utilization is associated with higher content of sp^2-coordinated carbon, which is a better electronic conductor than sp^3-coordinated and/or amorphous carbon, also present in these samples. Thus, the poorer performance of sol-gel samples compared to solid-state prepared 3A can be attributed to lower residual carbon content and to its highly disordered structure.

Figure 6 shows discharges of lithium cells containing doped samples, $Li_{0.98}Mg_{0.01}FePO_4$ (14SGA and 14SGB) and $Li_{0.96}Ti_{0.01}FePO_4$ (16SG). That of a cell containing 7SG is included for comparison. Although these samples were processed similarly (14SGA was planetary milled for only 15 minutes prior to the final firing, whereas the others were milled for 30 minutes), their discharge characteristics differ; low-level doping with Ti or Mg results in somewhat inferior performance, contrary to a previous report.[7]

If multivalent Mg^{2+} or Ti^{4+} is located in lithium sites, lithium ion diffusion may be hindered, further decreasing rate capability. Hydrothermally prepared $LiFePO_4$, in which ion-mixing occurs (i.e., some iron is in lithium sites), has poor electrochemical characteristics for this reason.[14] It is also possible that substitution was not successful in

these sol-gel prepared samples (small amounts of impurities are difficult to detect using x-ray diffraction experiments, and are essentially invisible if not crystalline). An examination of the surfaces of 14SGA and 14SGB by Raman spectroscopy shows the presence of contaminants not usually seen in typically pure sol-gel prepared samples, which may contribute to the lower utilization found in these samples.

In order to improve the rate capability of the sol-gel $LiFePO_4$ materials, we attempted to coat them with carbon by incorporating organic additives during the intermediate grinding step, after the initial decomposition at 500ºC. Samples were processed similarly to 7SG. Additives were chosen based on the following criteria: 1) tendency to decompose rather than evaporate at T≤600ºC, 2) solubility in acetone or another common solvent, to aid in dispersion over particle surfaces during milling, and 3) tendency to form cyclic compounds upon heating[15, 16] (4C and 5C) as shown below in equations 1 and 2, or the presence of aromatic or polyaromatic groups (1C, 2C, 3C, and 4C), all of which may act as templates for the formation of graphite precursors upon heating.[17]

(1) 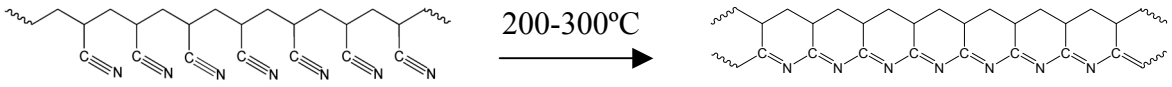

polyacrylonitrile (5C)

(2) 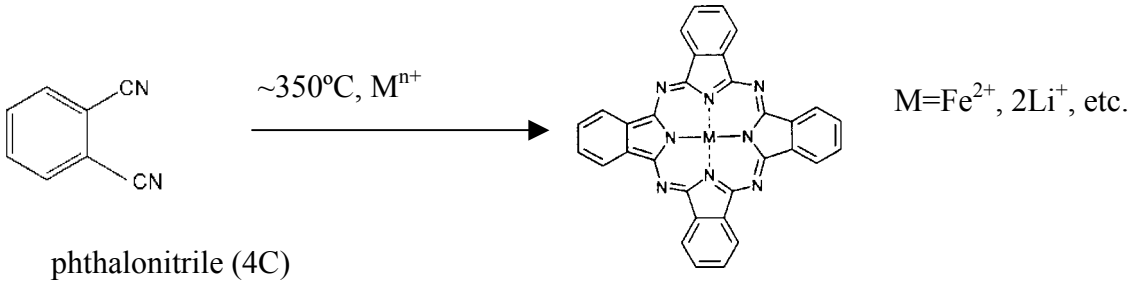

phthalonitrile (4C)

Despite the presence of additional amounts of carbon-containing additive, the final carbon content of the $LiFePO_4$ samples never exceeded 2 wt. % (Table 3) and, in some cases, was substantially less. This indicates that lower molecular weight compounds (pyromellitic acid (3C) and phthalonitrile (4C)) or their reaction products partially volatilize under the synthesis conditions. The presence of nitrogen in sample 4C (0.57 wt %) indicates, however, that phthalonitrile or phthalocyanine reaction product in equation 2 did not completely evaporate under the processing conditions used. Sample color varied from medium gray (4C) to deep black (1C).

The electrochemical capacity of the carbon coated $LiFePO_4$ in lithium cells at 0.055 mA/cm^2 (Figure 7) does not correlate with total carbon content. Interestingly, 3C (0.9 wt % C) and 1C (1.15 wt. % C) outperformed all other samples, including 3A (1.5 wt. % C). Improved utilization was obtained for most of the samples processed with additives when compared to 7SG (except for 4C). Figure 8 shows capacity as a function of current density for each type of cell (results from several cells were combined or averaged to construct the graph). This presents a more complicated picture, indicating that only 3C is clearly superior to 3A at all current densities tested. None of the electrodes could be utilized fully even at low discharge rates, and all showed a decrease in capacity as the current density was increased, indicating that there are still significant rate limitations. However, the rate of decrease, judging from the slopes of the lines in Figure 8, is less for the carbon coated samples (except 2C) than for 7SG.

Figure 9 shows micro-Raman spectra of the samples processed with organic additives (1-5C) compared to pristine 7SG and 3A powders. Two intense broad bands located at ~1350 cm^{-1} and ~1580 cm^{-1} dominated every spectrum of the $LiFePO_4$ samples

and can be assigned to the D and G bands of carbon, respectively. A weak band at 942 cm^{-1} corresponds to the symmetric vibration of the PO_4 group. All powder samples showed a quite uniform residual carbon distribution, which significantly screened the signal from $LiFePO_4$. We carried out a deconvolution analysis of the carbon bands to evaluate the content of sp^3 and sp^2 coordinated carbon in the samples as well as the degree of carbon disorder. We confirmed our earlier results, which showed that higher discharge capacities and better rate capability of $LiFePO_4$ cathodes are directly correlated with increased amounts of sp^2-type carbon domains and decreased level of disorder in graphene planes.[13] This effect can be explained in terms of the increasing amount of larger graphene clusters in the very disordered carbon structure, and, consequently, improved electronic conductivity of the carbon deposit. Improved electronic properties of the residual carbon can provide good electronic contact between sub-micron particles within large agglomerates, contributing to improved electrode performance.

In the case of 2C, symmetric stretch vibrations of -C=O and –C-O surface groups produced new bands that are close to the carbon G and D bands, respectively. Their effect on the Raman spectrum suggests that perylenetetracarboxylicdianhydride did not completely decompose under the processing conditions used in this study. The presence of excessive amounts of surface oxygen-containing functional groups on carbon can reduces surface electronic conductivity of carbon particles and/or account for unwanted side reactions with the electrolyte, and consequently, the inferior electrochemical behavior of this material. These bands were less evident in the Raman spectra of the better-performing 1C and 3C, which were coated using structural analogs with fewer

aromatic rings (naphthalenetetracarboxylicdianhydride and pyromellitic acid, respectively), suggesting a faster decomposition rate for these compounds.

Both 4C and 5C contain residual hydrogen and nitrogen (0.074% H, 0.57% N for 4C and 0.14% H and 1.10% N for 5C) indicating incomplete decomposition of the phthalonitrile and polyacrylonitrile used to coat the powders. The Raman spectra of nitrogen containing carbons show increased intensity of the peak 1350 cm^{-1} due to the contribution of vibrations of cyanate (OCN) groups. Phthalonitrile (4C) initially forms a (possibly semi-conducting) metallophthalocyanine compound upon heating (equation 2) but it is unlikely to survive heat-treatment at 600ºC. A thermal study of phthalocyanines and polyphthalocyanines[18] indicates an upper stability limit of about 400-600ºC in an inert atmosphere, depending upon the nature of M and other factors. Above the limit, bond cleavage occurs resulting in the release of HCN and other gases. Carbon films produced from polyacrylonitrile display a strong dependence of graphitic order and electronic conductivity on carbonization temperature.[15] Good conductivity can be attained only at temperatures above 900^{o}C.

In general, carbons produced by pyrolysis of organic or polymeric compounds at temperatures above 700ºC consist of more electronically conductive graphitic and less poorly conductive amorphous domains than those produced at lower temperatures.[15, 19] This presents a dilemma since undesirable particle growth of $LiFePO_4$ is rapid at 700ºC or above. Still, the differing D/G ratios obtained on the materials in this study suggest that the carbon structure can be manipulated to some extent by proper choice of organic precursors and processing conditions, even at 600ºC. For example, it may be possible to decrease the amount of residual nitrogen in the pyrolysis products of poly(acrylonitrile)

by heating samples under argon rather than nitrogen gas. At present, the factors influencing the structure of the carbon produced at 600ºC during synthesis of $LiFePO_4$ are not well understood. Nor do we know the optimal amount of carbon coating, which is likely to vary with the carbon structure, surface area of the $LiFePO_4$ powder, and other factors. Ideally, the amount of carbon should not exceed the maximum amount needed to be effective, so as not to compromise energy density unduly.

Alternatively, it might be possible to coat $LiFePO_4$ with a conductive substrate that can be made *in situ* at 500-600ºC. For example, room temperature conductivities as high as 1 S/cm have been reported for poly-copperphthalocyanine[20] synthesized under high pressure at 500ºC. It may be possible to produce this by coating $LiFePO_4$ particles with tetracyanobenzene and a copper salt before heating to the final temperature.

It should be noted, however, that slow diffusion of lithium ions across the $LiFePO_4/FePO_4$ two-phase boundary is another factor limiting performance of this material. Thus, it may still not be possible to produce a high-rate material simply by using a conductive coating, since this will not address the diffusivity problem. Although high rate capabilities have recently been reported for $LiFePO_4$,[7, 9] not all the details of the electrode configuration were specified. We have noticed better performance for very thin electrodes with high carbon contents (especially if expressed in term of C rates, rather than current densities), but these may not be practical for commercial use. Understanding the factors that go into making such a coating are, therefore, critical, and will be the focus of upcoming work in our laboratory.

Conclusions

Utilization of solid-state or sol-gel prepared $LiFePO_4$ samples used as cathodes in lithium cells depends primarily upon the structure of the residual carbon (0.5-2%) co-produced during the synthesis process. An increased amount of sp^2-coordinated carbon relative to sp^3-coordinated carbon on the $LiFePO_4$ surface is associated with better electronic conductivity and improved performance of the electrode. Carbon coatings with low D/G (disordered/graphene) ratios can be produced deliberately by adding small amounts of functionalized aromatic or ring-forming compounds before the final heating step in the sol-gel process. Significantly improved utilization and better rate capability was seen for several materials processed with additives, although the total carbon in the samples was lower than 2 wt. % (in some cases, less than 1 wt. %). Implications for electrode design are discussed.

Acknowledgments

This work was supported by the Assistant Secretary for Energy Efficiency and Renewable Energy, Office of FreedomCAR and Vehicle Technologies of the U.S. Department of Energy under Contract No. DE-AC03-76SF00098. Y. H. would like to thank the Department of Chinese Education for financial support. Some of this work was previously presented as Abstract 121 at the 202nd Meeting of the Electrochemical Society, Salt Lake City, UT October 2002.

References

1. A. K. Padhi, K. S. Nanjundaswamy, and J. B. Goodenough, *J. Electrochem. Soc.,* **144**, 1189 (1997).

2. A. S. Andersson, B. Kalska, L. Haggstrom, J. O. Thomas, *Solid State Ionics*, **130**, 41 (2000).

3. A. S. Andersson, B. Kalska, L. Haggstrom, J. O. Thomas, *Solid State Ionics*, **130**, 41 (2000).

4. A. Yamada, S. C. Chung and K. Hinokuma, *J. Electrochem. Soc.*, **148**, A224 (2001).

5. M. Takahashi, S. Tobishima, K. Takei, and Y. Sakurai, *J. Power Sources,* **97-98**, 508 (2001).

6. P. P. Prosini, M. Carewska, S. Scaccia, P. Wisniewski, S. Passerini, and M. Pasquali, *J. Electrochem. Soc.*, **149**, A886 (2002).

7. S.-Y. Chung, J. T. Blocking and Y.-M. Chiang, *Nature Materials,* **1**, 123 (2002).

8. F. Croce, A. D'Epifanio, J. Hassoun, A. Deptula, T. Olczac, and B. Scrosati, *Electrochem. and Solid State Letters,* **5**, A47 (2002).

9. H. Huang, S.-C. Yin, and L.F. Nazar, *Electrochem. and Solid State Letters*, **4**, A170 (2001).

10. N. Ravet, S. Besner, M. Simoneau, A. Vallee, M. Armand, J.-F. Magnan, European Patent Brevet EP 1 049 182 A2 , 2000.

11. Z. Chen and J. R. Dahn, *J. Electrochem. Soc.*, **149**, All84 (2002).

12. Y. Hu, Y. J. Lee, M. M. Doeff, E. J. Cairns and J. A. Reimer, unpublished results.

13. M. M. Doeff, Y. Hu, F. McLarnon, and R. Kostecki, *Electrochem. and Solid State Letters,* in press, 2003.

14. S. Yang, Y. Song, P. Y. Zavalij, and M. S. Whittingham, *Electrochem. Commun.,* **4**, 239 (2002).

15. C. L. Renschler, A. P. Sylwester, and L.V. Salgado, *J. Mater. Res.,* **4**, 452 (1989).

16. N. B. McKeown, *J. Mater. Chem.,* **10**, 1979 (2000).

17. K. Kamiya, T. Noda, M. Ide, and J. Tanaka, *Synth. Met.* **71**, 1765 (1995).

18.. D. Wöhrle and B. Schulte, *Makromol. Chem.*, **186**, 2229 (1985).

19. R. Kostecki, B. Schynder, D. Alliata, X. Song, K. Kinoshita and R. Kötz, *Thin Solid Films,* **396**, 36 (2001).

20. K. Yakushi, I. Shirotani, I. I. Khairullin, Y. Nakazawa, K. Kanoda, N. Kosugi, and S. Takeda, *Synth. Met.*, **71**, 2287 (1995).

Table 1. Process Parameters for $LiFePO_4$ Samples

Sample	Composition	Synthesis method[a]	Processing parameters		
			1st heating	Grinding[b]	2nd heating
3A	$LiFePO_4$	Solid state	300 ºC, 10 h	30 min.	600 ºC, 8 h
3SG	$LiFePO_4$	Sol-gel	600 ºC, 6 h, no grinding		
6SG	$LiFePO_4$	Sol-gel	500 ºC, 10 h	1 h[c]	700 ºC, 10 h
7SG	$LiFePO_4$	Sol-gel	500 ºC, 10 h	30 min.	600 ºC, 10 h
8SG	$LiFePO_4$	Sol-gel	500 ºC, 10 h	—[d]	600 ºC, 10 h
9SG	$LiFePO_4$	Sol-gel	500 ºC, 10 h	45 min.	700 ºC, 10 h
10SG	$LiFePO_4$	Sol-gel	500 ºC, 10 h	45 min.	700 ºC, 10 h[e]
12SGA	$LiFePO_4$	Sol-gel	500 º C, 10 h	30 min.	600 ºC, 5 h
12SGB	$LiFePO_4$	Sol-gel	500 º C, 10 h	1 h	600 ºC, 5 h
14SGA	$Li_{0.98}Mg_{0.01}FePO_4$	Sol-gel	500 º C, 10 h	15 min.	600 ºC, 10 h
14SGB	$Li_{0.98}Mg_{0.01}FePO_4$	Sol-gel	500 º C, 10 h	30 min.	600 ºC, 10 h
15SG	$LiFePO_4$	Sol-gel	500 º C, 10 h	30 min.	600 ºC, 15 h
16SG	$Li_{0.96}Ti_{0.01}FePO_4$	Sol-gel	500 º C, 10 h	30 min.	600 ºC, 10 h

a) See experimental section for details

b) planetary milled in acetone except where otherwise noted

c) planetary milled without solvent

d) hand-ground

e) planetary milled in acetone one hour after final heating

Table 2. $LiFePO_4$ samples processed with organic additives.[a]

Sample	Additive	Structure of additive
1C	naphthalenetetracarboxylicdianhydride	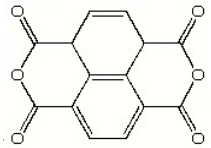
2C	perylenetetracarboxylicdianhydride	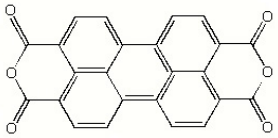
3C	pyromellitic acid	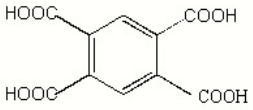
4C	phthalonitrile	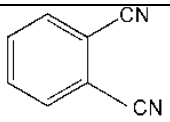
5C	Poly(acrylonitrile)	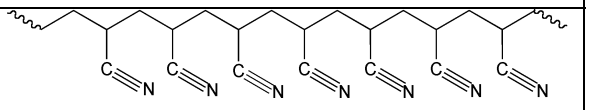

a) Processing variables identical to 7SG in Table 1. Organic compounds were added during the intermediate grinding step, before firing at 600ºC.

Table 3 Carbon content and mean particle size for $LiFePO_4$ samples

Sample	Carbon content (wt %)	Mean primary particle size, (μm)
3A	1.47	17
3SG	0.574	~20[a]
6SG		59
7SG	0.690	7
8SG		42
9SG		110
10SG	0.495	5
12SGA		5.5
12SGB	0.507	4.5
14SGB	0.298	
15SG	0.400	9.9
16SG	0.452	
1C	1.15	
2C	1.49	8.2
3C	0.906	
4C	0.51	
5C	1.99	

a) estimated from scanning electron micrographs.

Figure Captions

Figure 1. Scanning electron micrographs of $LiFePO_4$ powders: a) 3A, b) 7SG, c) 6SG, and d) 8SG.

Figure 2. Cyclic voltammograms of Li/1M $LiPF_6$, EC-DMC/$LiFePO_4$ cells containing samples 3A (—), 7SG (- - -), 10SG (·····), and 12SGA (—x). Scan rate 0.05 mV/sec.

Figure 3. Electrochemical discharge capacity of Li/1M $LiPF_6$, EC-DMC/$LiFePO_4$ cells, as a function of $LiFePO_4$ mean primary particle size. See Table 1 for sample codes.

Figure 4. Galvanostatic discharges at 0.027 mA/cm^2 of Li/1M $LiPF_6$, EC-DMC/$LiFePO_4$ cells containing samples 3A (—), 7SG (▪▪▪▪), 15SG (-----), 10SG (·····), 12SGA (—x) and 12SGB (···+···).

Figure 5. a) Galvanostatic discharges of a Li/1M $LiPF_6$, EC-DMC/3A-$LiFePO_4$ cell at 0.055 mA/cm^2 (—), 0.11 mA/cm^2 (-----) and 0.22 mA/cm^2 (·····). b) Discharges of a Li/1M $LiPF_6$, EC-DMC/7SG-$LiFePO_4$ cell at 0.027 mA/cm^2 (—), 0.055 mA/cm^2 (-----) and 0.11 mA/cm^2 (·····).

Figure 6. Galvanostatic discharges at 0.027 mA/cm^2 of lithium cells containing samples 7SG, $LiFePO_4$ (—), 14SGB, $Li_{0.98}Mg_{0.01}FePO_4$ (▪▪▪▪), 16SG, $Li_{0.96}Ti_{0.01}FePO_4$ (-----) and 14SGA, $Li_{0.98}Mg_{0.01}FePO_4$ (·····).

Figure 7. Galvanostatic discharges at 0.055 mA/cm^2 of lithium cells containing samples 3C(—), 1C(---), 3A (·····), 5C (—x), 7SG (—+), 2C (—○) and 4C (— —).

Figure 8. Electrochemical discharge capacity as a function of current density for lithium cells containing samples 3C (x), 3A (□), 1C (▲), 5C (●), 7SG (+), 2C (◇), and 4C (○). Points represent averages of data taken from several different cells of each type.

Figure 9. Raman spectra of $LiFePO_4$ powders.

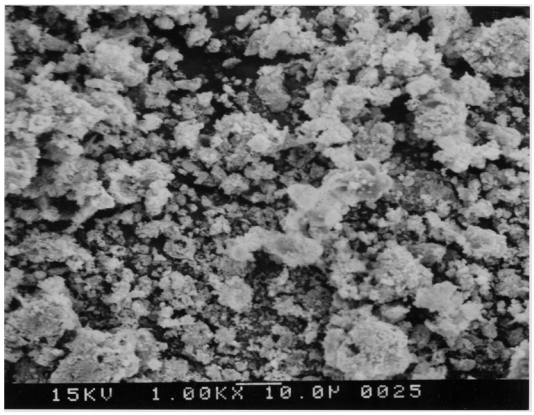

a

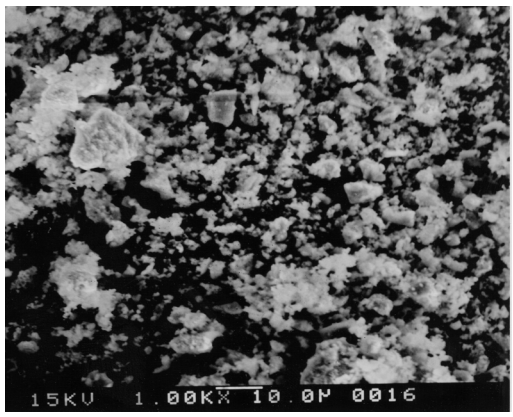

b

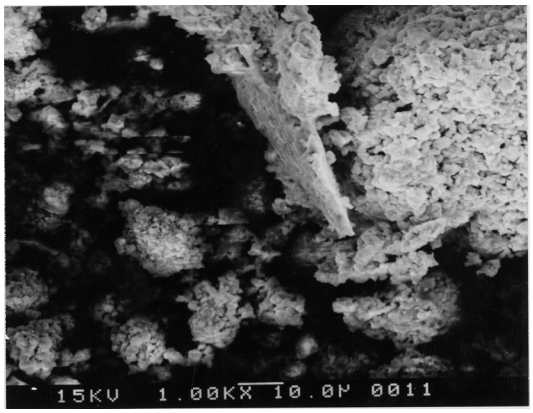

c

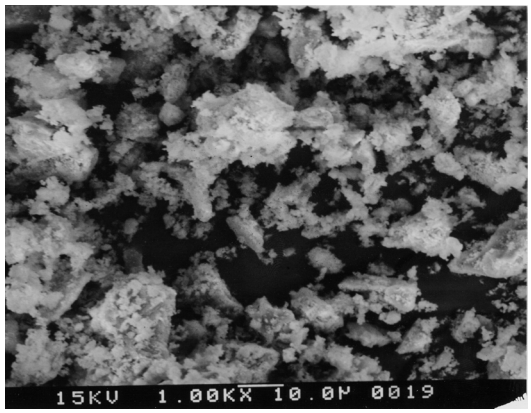

d

Figure 1

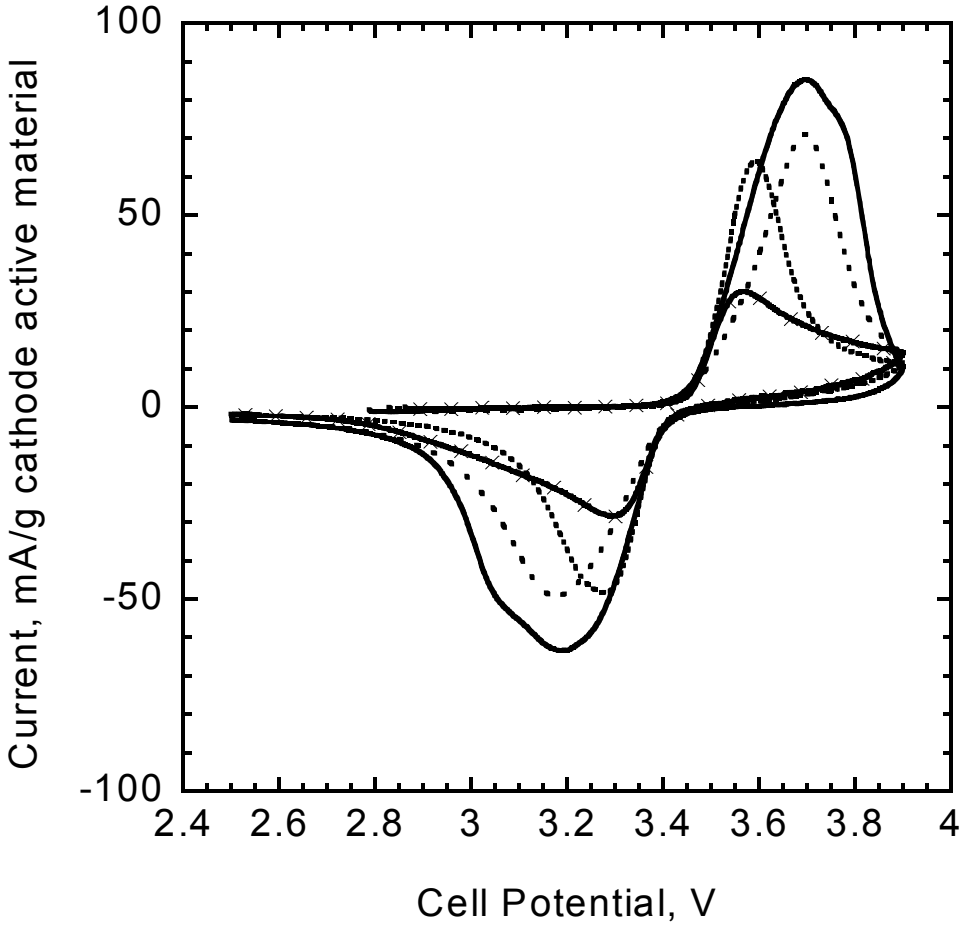
100
50
0
-50
-100
2.4
2.6
2.8
3
3.2
3.4
3.6
3.8
4
Current, mA/g cathode active material
Cell Potential, V

Figure 2

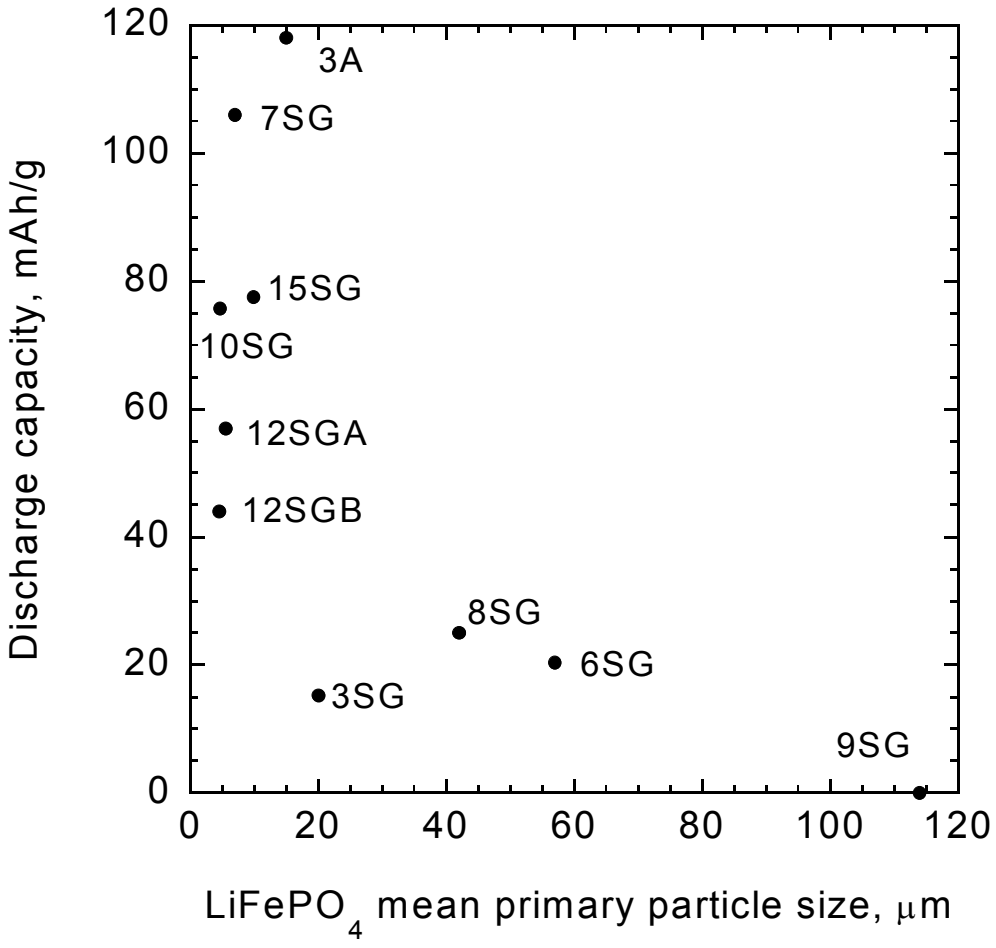
120
100
80
60
40
20
0
0
20
40
60
80
100
120
Discharge capacity, mAh/g
LiFePO4 mean primary particle size, μm
3A
7SG
15SG
10SG
12SGA
12SGB
8SG
6SG
3SG
9SG

Figure 3.

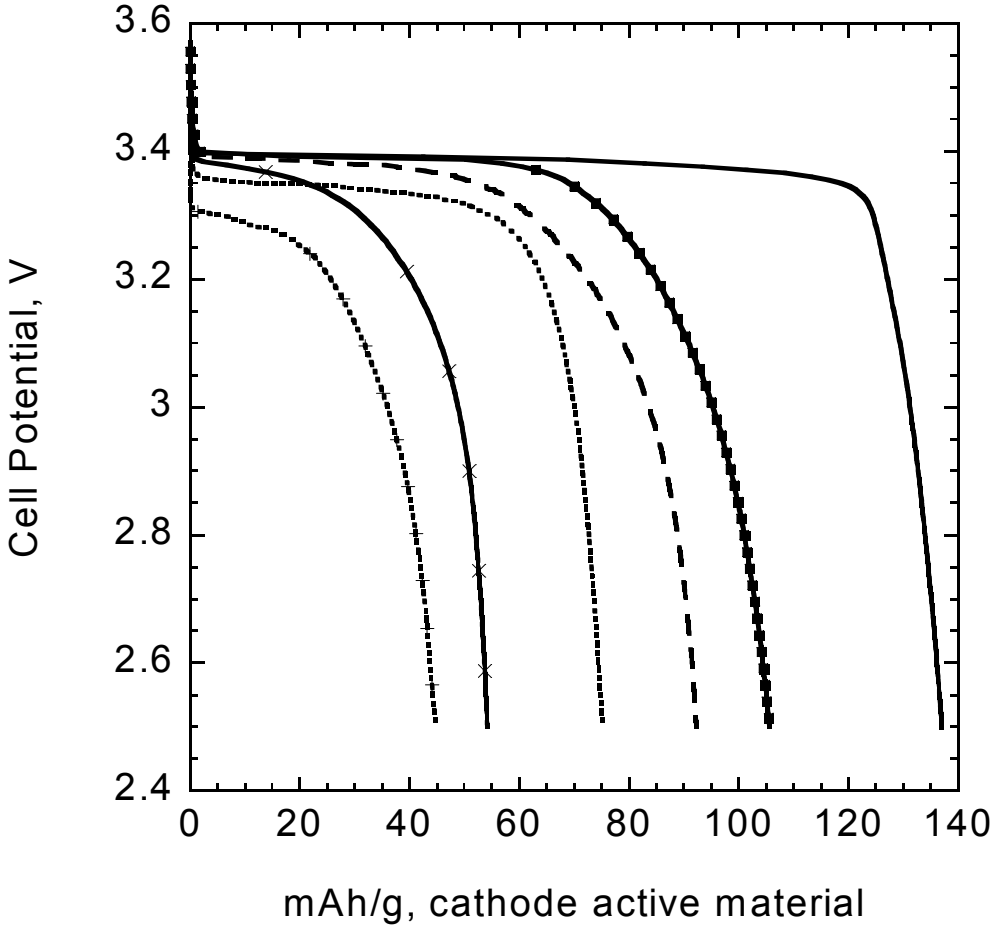
3.6
3.4
3.2
3
2.8
2.6
2.4
Cell Potential, V
0
20
40
60
80
100
120
140
mAh/g, cathode active material

Figure 4

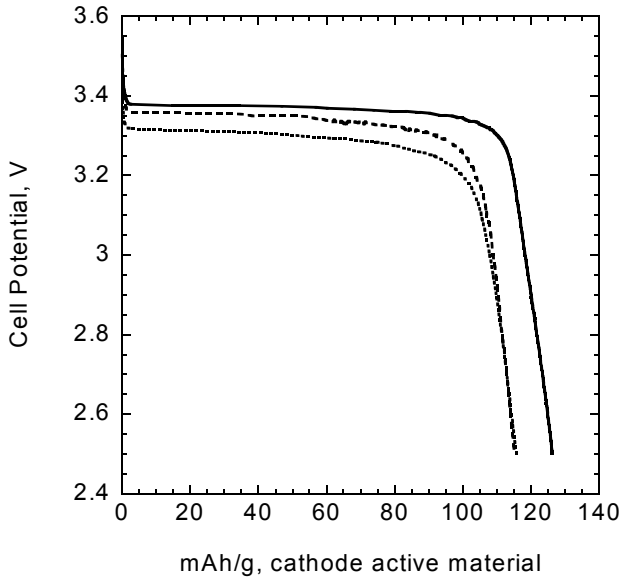
3.6
3.4
3.2
3
2.8
2.6
2.4
Cell Potential, V
0
20
40
60
80
100
120
140
mAh/g, cathode active material

a

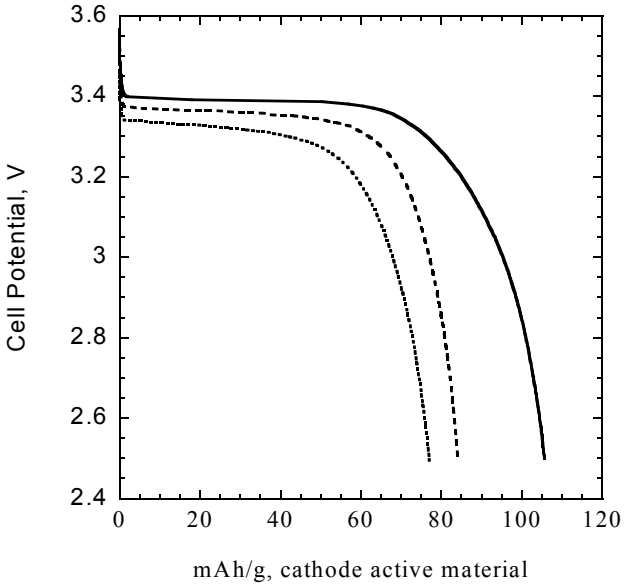
3.6
3.4
3.2
3
2.8
2.6
2.4
Cell Potential, V
0
20
40
60
80
100
120
mAh/g, cathode active material

b

Figure 5

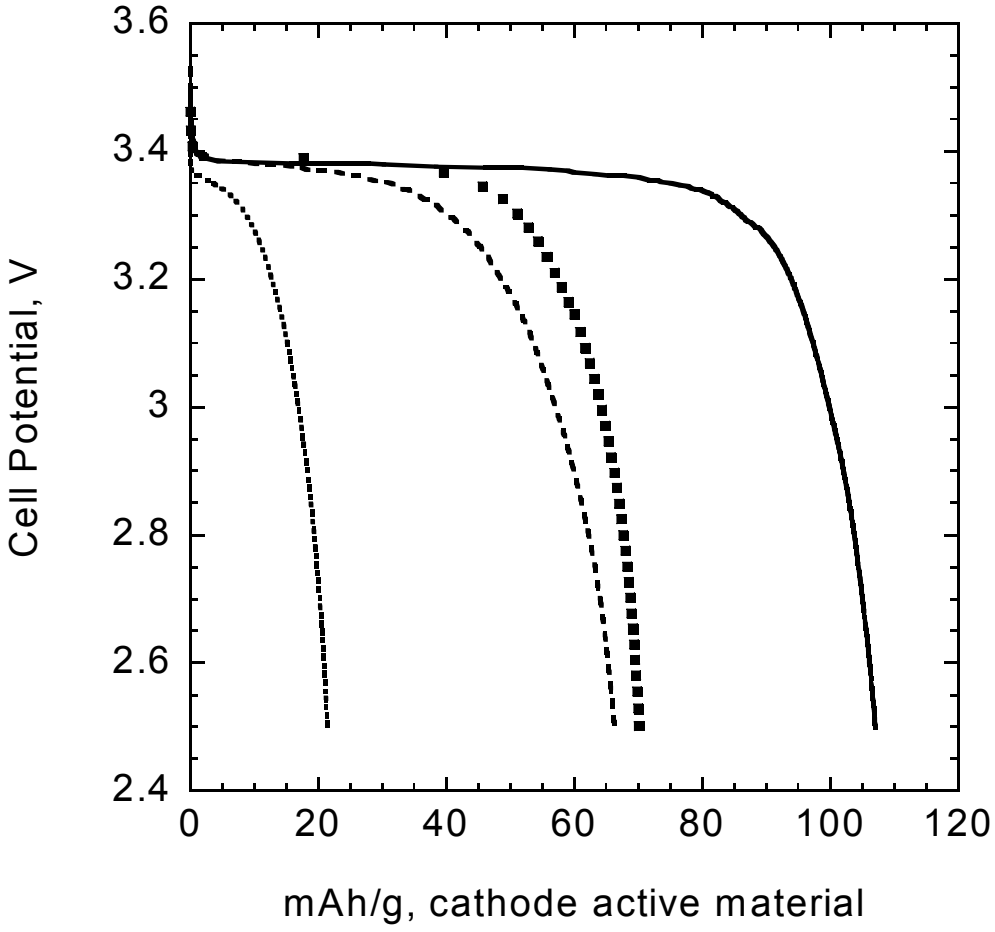
3.6
3.4
3.2
3
2.8
2.6
2.4
Cell Potential, V
0
20
40
60
80
100
120
mAh/g, cathode active material

Figure 6

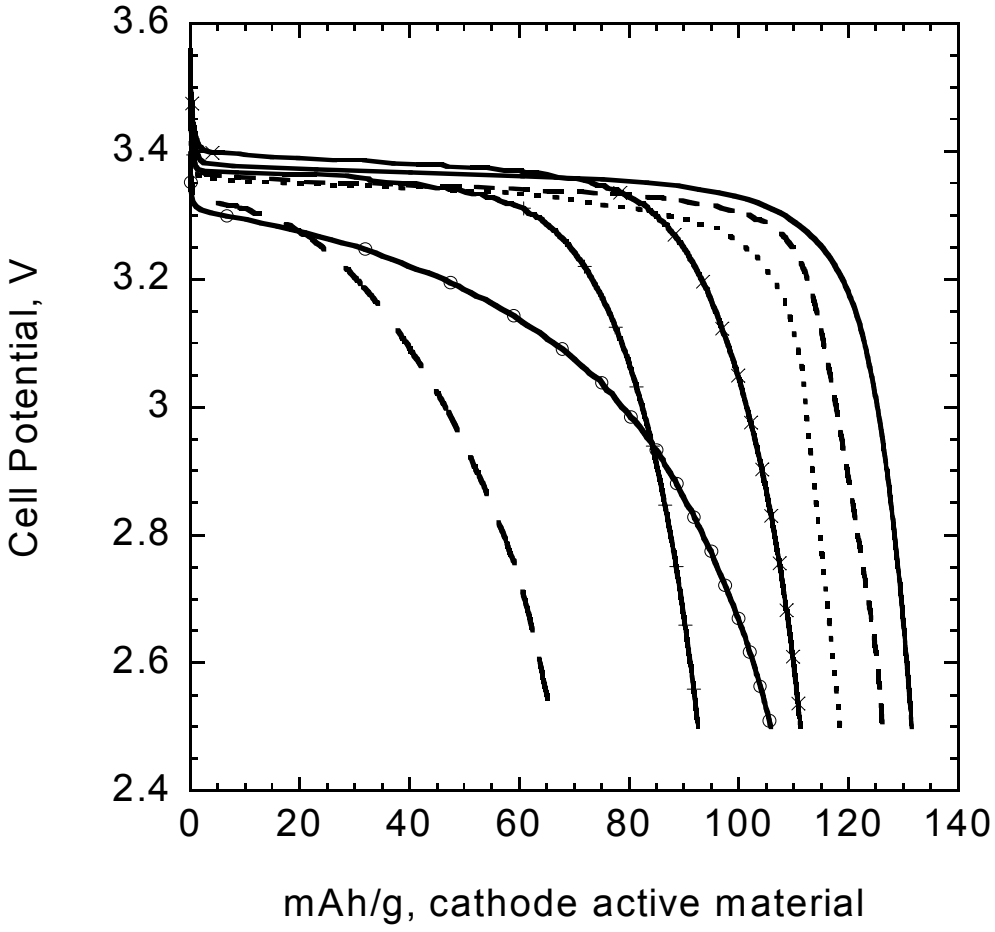
3.6
3.4
3.2
3
2.8
2.6
2.4
Cell Potential, V
0
20
40
60
80
100
120
140
mAh/g, cathode active material

Figure 7.

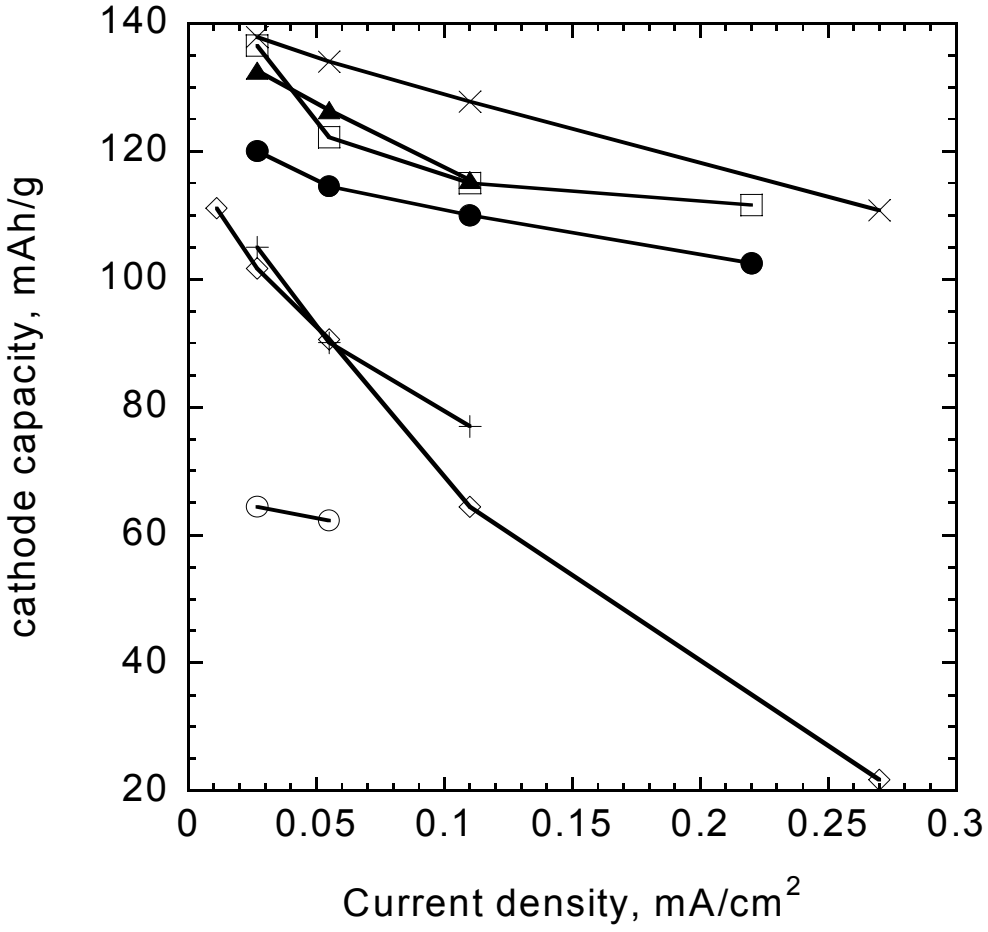
140
120
100
80
60
40
20
0
0.05
0.1
0.15
0.2
0.25
0.3
cathode capacity, mAh/g
Current density, mA/cm2

Figure 8.

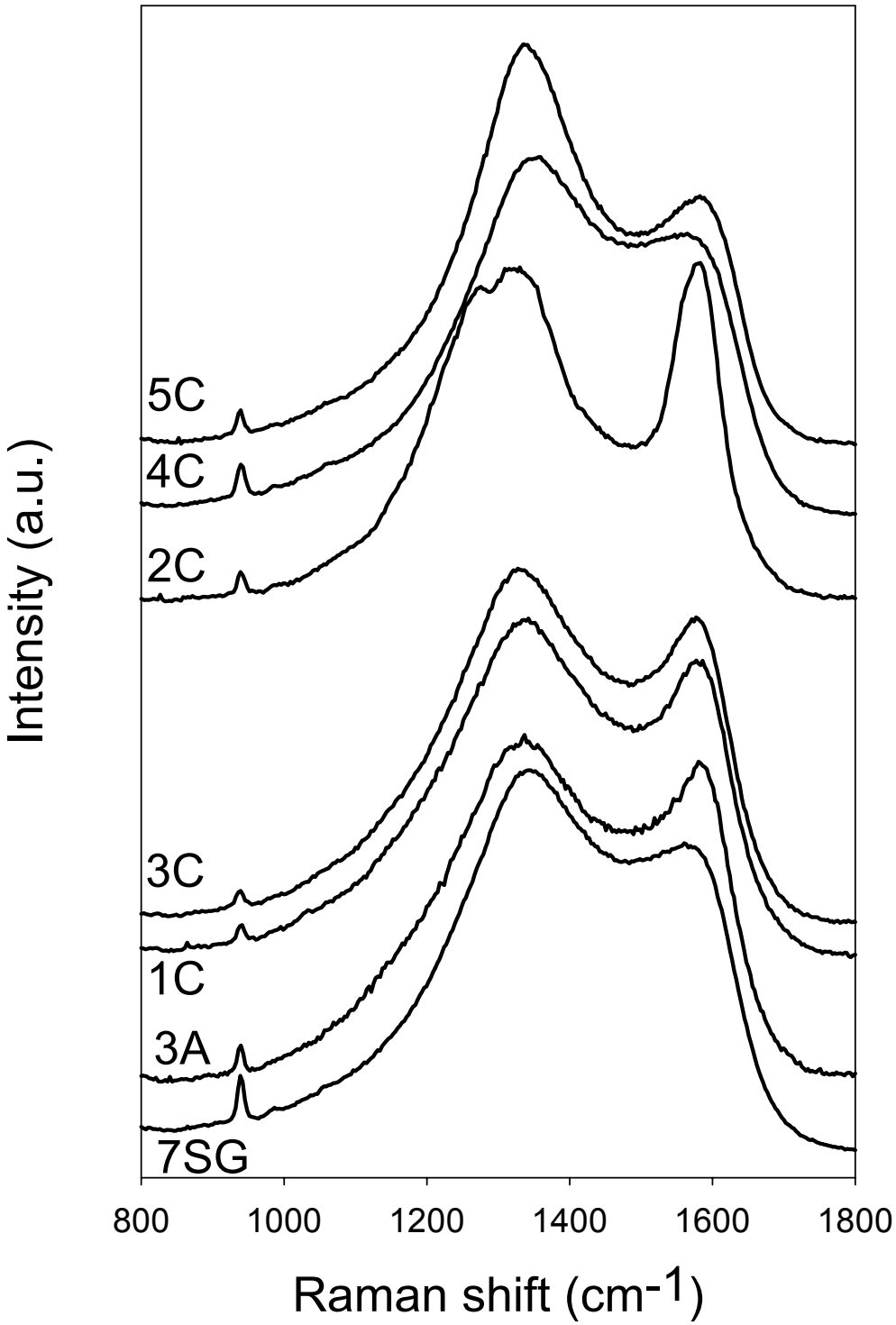
5C
4C
2C
3C
1C
3A
7SG
Intensity (a.u.)
800
1000
1200
1400
1600
1800
Raman shift (cm-1)

Figure 9